J Fluoresc (2010) 20:143–151
DOI 10.1007/s10895-009-0532-5

ORIGINAL PAPER

Fluorescent Properties of a Hybrid Cadmium Sulfide-Dendrimer Nanocomposite and its Quenching with Nitromethane

Bruno B. Campos · Manuel Algarra · Joaquim C. G. Esteves da Silva

Received: 26 June 2009 / Accepted: 7 August 2009 / Published online: 2 September 2009

Abstract A fluorescent hybrid cadmium sulphide quantum dots (QDs) dendrimer nanocomposite (DAB-CdS) synthesised in water and stable in aqueous solution is described. The dendrimer, DAB-G5 dendrimer (polypropylenimine tetrahexacontaamine) generation 5, a diaminobutene core with 64 amine terminal primary groups. The maximum of the excitation and emission spectra, Stokes' shift and the emission full width of half maximum of this nanocomposite are, respectively: 351, 535, 204 and 212 nm. The fluorescence time decay was complex and a four component decay time model originated a good fit (χ=1.20) with the following lifetimes: τ_1=657 ps; τ_2=10.0 ns; τ_3=59.42 ns; and τ_4=265 ns. The fluorescence intensity of the nanocomposite is markedly quenched by the presence of nitromethane with a dynamic Stern-Volmer constant of 25 M^{-1}. The quenching profiles show that about 81% of the CdS QDs are located in the external layer of the dendrimer accessible to the quencher. PARAFAC analysis of the excitation emission matrices (EEM) acquired as function of the nitromethane concentration showed a trilinear data structure with only one linearly independent component describing the quenching which allows robust estimation of the excitation and emission spectra and of the quenching profiles. This water soluble and fluorescent nanocomposite shows a set of favourable properties to its use in sensor applications.

Keywords Dendrimers · CdS quantum dots · Fluorescence · Quenching · Nitromethane

B. B. Campos · J. C. G. Esteves da Silva (✉)
Centro de Investigação em Química, Departamento de Química,
Faculdade de Ciências da Universidade do Porto,
R. Campo Alegre 687,
4169-007 Porto, Portugal
e-mail: jcsilva@fc.up.pt

M. Algarra
Centro de Geologia do Porto, Faculdade de Ciências,
Universidade do Porto,
Rua do Campo Alegre 687,
4169-007 Porto, Portugal

Introduction

The discover of luminescent semiconductor nanocrystals, also known as quantum dots (QDs), lead to extensive research in several areas of science [1–5]. Due to their unique and excellent luminescent properties, QDs have demonstrated several remarkable and attractive optoelectronic characteristics especially suited to analytical and bioanalytical applications [6–8] The synthesis of water soluble and stable derivates of QDs markedly open the research to new applications, for example, sensing [9–17], diagnosis [18, 19], imaging [20] and optical tracking [21].

Surface modification of QDs is particularly important in sensor designing, where the conjugation of suitable recognition groups will target an analyte, creating a hybrid QD-receptor sensing system. Dendrimers are artificial polymers, which combine the typical characteristics of small organic molecules, like defined composition and monodispersivity, with those of polymers, such as high molecular weight that results in multitude of physical properties [22–24]. The coating of QDs, rendering them biocompatibility and biostability, confers an important biomedical role in diagnostics and biochemical sensing [25–27]. Moreover, dendrimers are a particularly interesting class of emerging nanopharmaceuticals [28].

The most used dendrimer for QDs capping are of the poly(amidoamine) type (PAMAM) polymers [29–34]. Hybrid CdS QDs and PAMAM nanocomposites have been proposed for fingerprint detection [33], discrimination of drugs [35] and proteins [36] or DNA analysis [37]. Dendrimers of the (polypropylenimine tetrahexacontaamine) type (DAB) in methanol solution have been used as capping agents for CdS QDs [31, 32].

In this paper, the synthesis of a hybrid cadmium sulphide quantum dots (QDs) dendrimer (DAB, generation 5) nanocomposite (DAB-CdS) in water is described. The synthesised nanocomposite (DAB-CdS) is stable in aqueous solution and its steady state and lifetime fluorescent properties will be presented and discussed. Also, the quenching of the fluorescence of DAB-CdS by nitromethane is presented and analysed using Stern-Volmer models and PARAFAC (parallel factor analysis) method. PARAFAC is a chemometric multi-way decomposition method particularly suitable for the analysis of excitation emission matrices (EEM) [15, 16, 38–43].

Experimental section

Reagents

DAB-G_5 dendrimer (polypropylenimine tetrahexacontaamine) generation 5 (diaminobutene core and 64 amine terminal primary groups, Fig. 1), cadmium chloride ($CdCl_2$, 99.9%), sodium sulphide and 3-mercaptopropinoic acid (MPA) (Fluka, 99%) were obtained from Sigma-Aldrich Química S. A. (Spain). All solutions were made with deionised water with resistivity higher than 4 MΩ/cm.

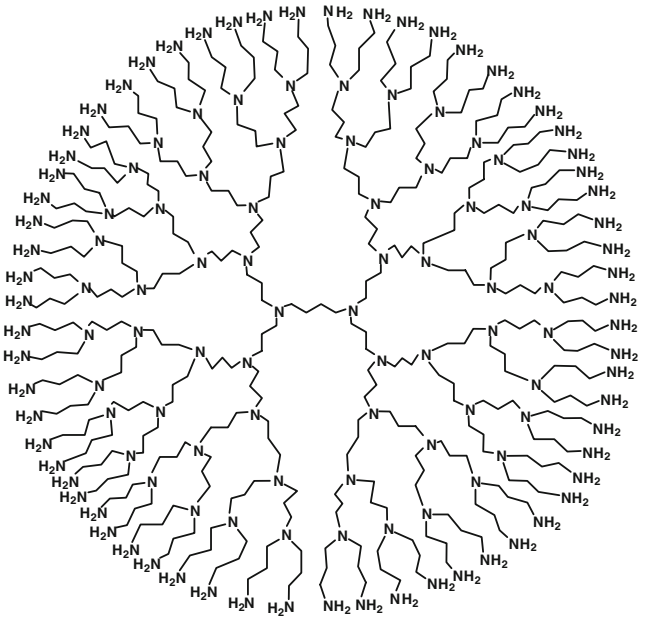

Fig. 1 Molecular structure of DAB-G5

Synthesis of DAB-CdS QDs

The synthesis procedure uses 85.1 mg of DAB-G_5 (0.0119 mmol) dissolved in water (170 mL) with continuously stirring for 24 h. After that, 21.9 mg of $CdCl_2$ (0.119 mmol) was added and left to stabilize for about 24 h. 850 μL (9.70 mmol) of MPA was added and left to stabilize during 24 h. Equimolar sodium sulfide (0.129 mmol) was then added and stirred for 72 h to afford a transparent solution that was dialyzed using a MW CO 12,000–14,000 Dalton dialysis tube (Medicell International) for 12 h against deionized water at room temperature. After dialysis the solution was centrifuged at 13,000 rpm for 10 min to remove suspended solids. The obtained solution of DAB-CdS QDs was used for further experiments.

The DAB-CdS solution, kept at room temperature and protected from light, was stable in aqueous solution and its fluorescent properties do not show marked variation for at least three months.

DAB-CdS/nitromethane mixtures

Rigorous aliquots of nitromethane were added to a 5 mL volumetric flask with 3 mL of DAB-CdS solution and the meniscus adjusted with deionizer water. Nitromethane concentration in the DAB-CdS solutions were: 0.00365 M; 0.0365 M; 0.0730 M; 0.109 M; 0.146 M; 0.182 M; 0.219 M.

Instrumentation

Excitation emission matrices of fluorescence (EEM) [excitation between 199.4 and 672.8 nm and emission between 349.7 and 719.7 nm] were obtained with a Spex 3D luminescence spectrophotometer equipped with a Xenon pulse discharge lamp (75 W) and a CCD detector, 0.25 mm slits and 1 s integration time were used. Lifetime measurements were recorded with a Horiba Jovin Yvon Fluoromax 4 TCSPC using the following instrumental settings: 368 nm NanoLED; time range, 1.6 μs; peak preset; 10,000 counts; repetition rate, 500 kHz; synchronous delay, 25 ns; emission detection: 535 nm. Quartz cuvettes were used.

Energy dispersive X-Ray analysis (EDS) of the three purified QDs were done on a FEI Quanta 400FEG/EDAX Genesis X4M high resolution scanning electronic microscope. For EDS analysis the DAB-CdS solution was evaporated under vacuum at room temperature and placed in an aluminum support. Absorbance measure-

ments were made in a Hewlett-Packard HP8452A diode-array spectrophotometer.

Data analysis

Lifetime deconvolution analysis was done using Decay Analysis Software v6.4.1 (Horiba Jovin Yvon). Fluorescence decays were interpreted in terms of a multiexponential model:

$$I(\mathrm{t}) = \mathrm{A} + \Sigma\, \mathrm{B_i}\ \exp(-t/\tau_\mathrm{i}) \tag{1}$$

where B_i are the preexponential factors and τ_i the decay times. The fraction contribution (percentage of photons) of each decay time component is represented by P_i.

In this study collisional quenching of fluorescence by nitromethane was described using the Stern-Volmer equation:

$$\mathrm{Io/I} = 1 + K_\mathrm{D}[\mathrm{nitromethane}] \tag{2}$$

where Io is the fluorescence intensity without nitromethane, I is the fluorescence intensity observed in the presence of nitromethane and K_D is the dynamic (collisional) Stern-Volver constant. The quenching was also described by a modified Stern-Volmer equation accounting for a fractional accessibility to quenchers:

$$\mathrm{Io}/\Delta\mathrm{I} = 1/(f\mathrm{a}\ K_\mathrm{a}[\mathrm{nitromethane}] + 1/f\mathrm{a} \tag{3}$$

where $\Delta I = (Io-I)$, f_a is the fraction of initial fluorescence that is accessible to quencher and K_a is the Stern-Volmer quenching constant of the accessible fraction.

The PARAFAC models a three-way tri-linear data structure $\mathbf{X}(i\times j\times k)$ with elements x_{ijk} corresponds to the product of three matrices $\mathbf{A}(i\times n)$, $\mathbf{B}(j\times n)$ and $\mathbf{D}(k\times n)$ plus the matrix of error ($\mathbf{E}(i\times j\times k)$). Each element x_{ijk} can be calculated by:

$$x_{ijk} = \sum_{n=1}^{N} a_{in}b_{jn}d_{kn} + e_{ijk} \tag{4}$$

where a_{in}, b_{jn}, c_{kn} and e_{ijk} are respectively the elements of the **A**, **B**, **D** and **E** matrices. If the EEM folows a trilinear model (number of components equals the number of fluorophores) then the PARAFAC solution (a, b and d) should be equivalent to the physico-chemical quantities (quenching profiles, exitation and emission spectra).

The results obtained from the different PARAFAC models were compared using the model fit [Fit (%)] defined by Eq. 5 [43]:

$$\mathrm{Fit}(\%) = 100 \times \left(1 - \sqrt{\frac{\sum_{i=1}^{I}\sum_{j=1}^{J}\sum_{k=1}^{K}\left(f_{ijk} - x_{ijk}\right)^2}{\sum_{i=1}^{I}\sum_{j=1}^{J}\sum_{k=1}^{K}\left(f_{ijk}\right)^2}}\right) \tag{5}$$

Also, the results obtained with PARAFAC models are assessed using the corcondia test defined by Eq. 6 [43]:

$$\mathrm{Corcondia}(\%) = 100 \times \left(1 - \frac{\sum_{d=1}^{N}\sum_{e=1}^{N}\sum_{f=1}^{N}\left(g_{def} - t_{def}\right)^2}{\sum_{d=1}^{N}\sum_{e=1}^{N}\sum_{f=1}^{N}\left(t_{def}\right)^2}\right) \tag{6}$$

In this equation g_{efg} and t_{efg} denote the elements of the calculated core and of the intrinsic super-diagonal core, respectively, and N the number of components of the model. If they are equal, the core consistency is perfect and has a value of unity (100%). Models with a corcondia value signifcantly lower than 100% should not be considered.

For PARAFAC analysis raw EEM were reduced to an excitation wavelength range from 288 to 382 nm (46 data points) and an emission wavelength range from 432 to 680 nm (121 data points). Experimental data matrices were arranged as a three dimensional array [nitromethane concentrations × emission (nm) × excitation (nm)]—a typical dimension was (7, 121, 46). Data analysis was performed in MATLAB version 7.5.0.342. The PARAFAC code was obtained from http://www.models.kvl.dk/source/nwaytoolbox.

Results and discussion

EDS/SEM and absorption spectra of DAB-CdS

Figure 2a and b shows the EDS spectrum and a SEM image of the purified DAB-CdS. The presence of the signals in the EDS spectrum due to elements Cd and S confirms the presence of the QDs; C and N are due to DAB capping the QDs; the detection of the elements O, C and S suggests that MPA is also capping the QDs and contribute to their stabilization. SEM images (Fig. 2b shows an example) do not give information about the morphology of the material but amorphous structures with several hundreds nm can be observed.

Figure 2c shows the absorption spectrum of DAB-CdS in water. The analysis of the spectrum shows the existence of a broad absorption band in the wavelength range between 300 and 400 nm. A detailed analysis of this band suggests that it result from the overlapped of at least two bands with maximum absorbance at 325 and 375 nm. This existence of absorption bands in this wavelength range is characteristic of QDs with nanometre diameter sizes [32]. The existence of an absorption broad band suggests a relatively high heterogeneity of the sizes of the CdS QDs capped with DAB and MPA.

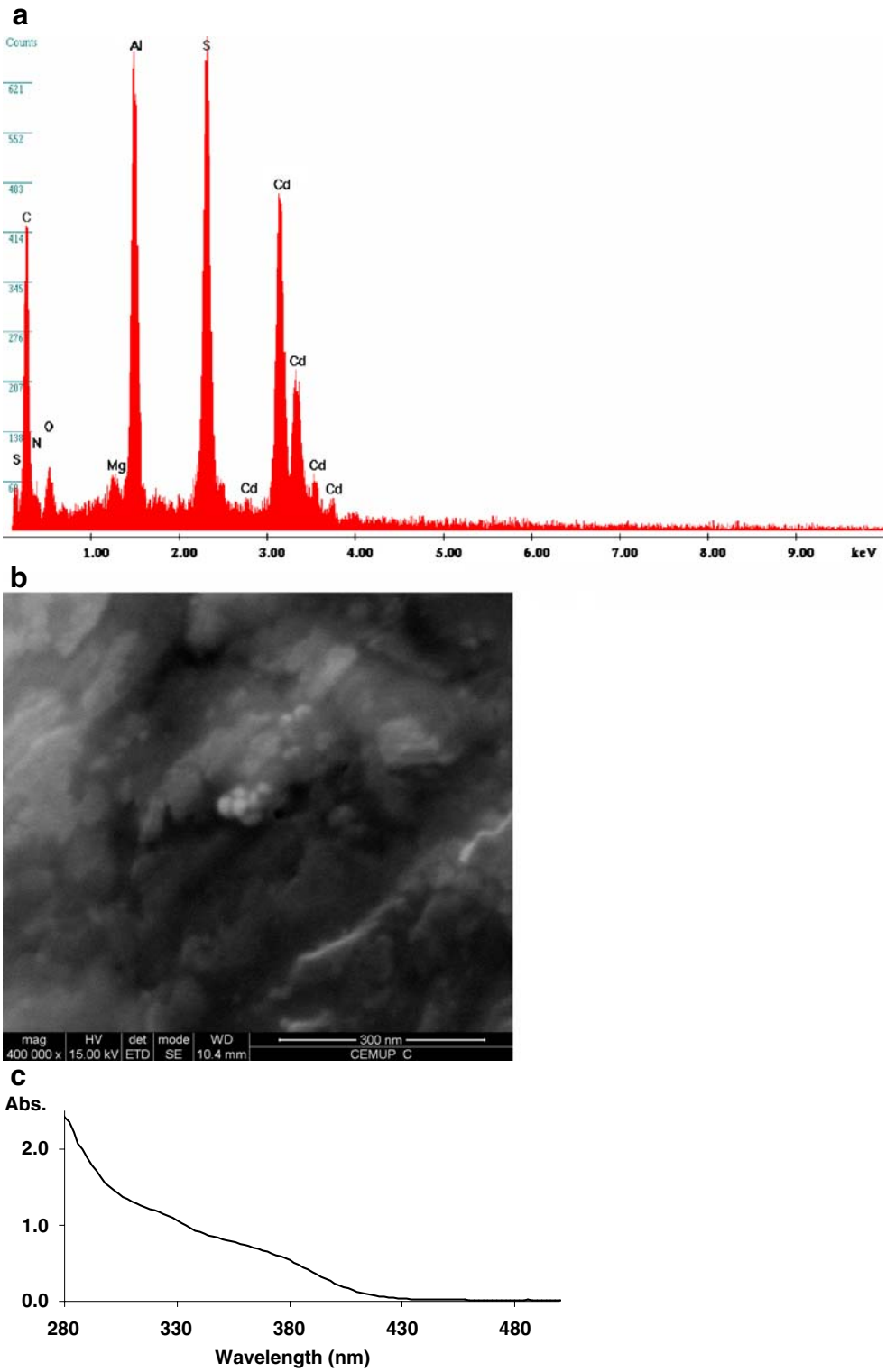

Fig. 2 EDS spectra (**a**), SEM image (**b**) and room temperature absorption spectra of DAB-CdS in water (**c**)

Steady state fluorescence

Figure 3a shows a typical EEM of aqueous solutions of DAB-CdS. This nanoparticle is fluorescent showing maximum excitation and emission at 351 and 535 nm, respectively. The analysis of the EEM also shows that the maximum of the emission spectra is not dependent on the excitation wavelength as observed in other dendrimer-CdS nanocomposites [30]. This result shows that this substance has a relatively high Stokes' shift of 204 nm.

The emission full width of half maximum (fwhm) is 212 nm which is a relatively high value when compared with typical narrow emission bands of QDs. This relatively high fwhm suggests that the fluorophores (CdS QDs) show a high degree of size and shape heterogeneity when bounded to the dendrimer. Indeed, this property is typical of colloidal CdS QDs, as well of their nanocomposites with organic molecules [30–32].

The effect of the dendrimer capping on the fluorescence intensity (quantum yield) of CdS QDs could not be rigorously study because the repetition of the described synthesis (Experimental section) without DAB failed to obtain CdS QDs. CdS QDs could only be obtained with higher MPA concentrations and after adjusting the pH of the solution before the addition of sulphide to 6.5. The comparison of the fluorescence intensity of the two CdS

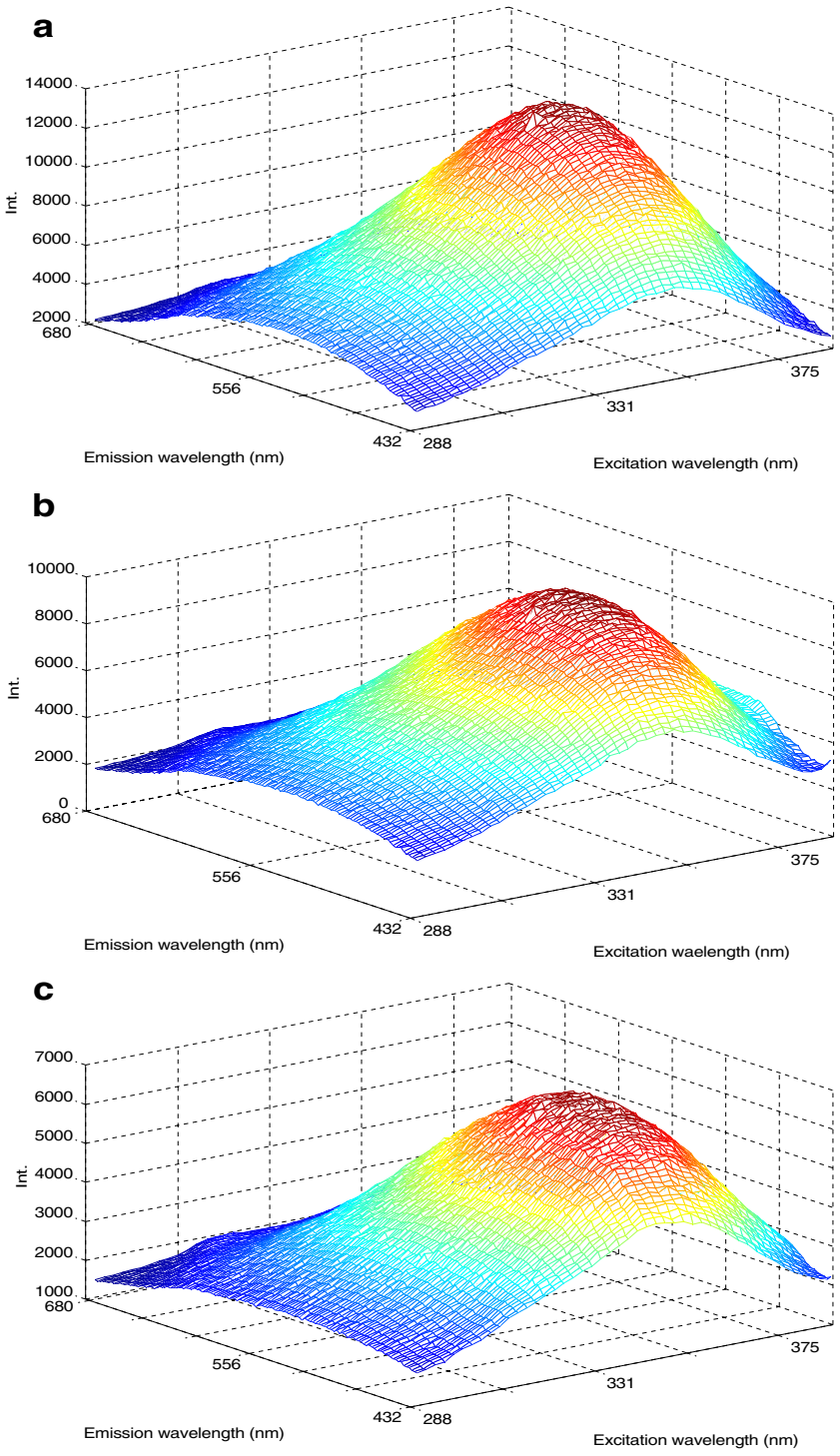

Fig. 3 Excitation emission matrices of fluorescence of aqueous solutions of DAB-CdS without (**a**) and with nitromethane: 0.0365 M (**b**) and 0.109 M (**c**)

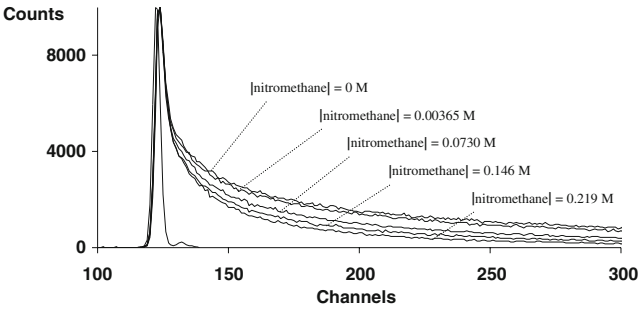

Fig. 4 Fluorescence decays of aqueous solutions of DAB-CdS in the presence of increasing concentrations of nitromethane

QDs (without and with DAB) showed that the CdS QDs capped with DAB were about four times more fluorescent that the MPA capped CdS QDs. This enhancement of the fluorescence of CdS QDs by dendrimers has already been described in the literature [32].

The synthesized DAB-CdS nanocomposite show a similar emission maximum to literature reports of mercaptoacetic acid-capped-CdS (541 nm) [44], dendrimer-encapsulated CdS nanoparticles (465 to 480 nm [31]) (470 to 510 nm [32]).

Lifetime analysis

Typical fluorescence time decay profiles of DAB-CdS are shown in Fig. 4. The preliminary analysis of the time decay shows that it is complex showing the presence of lifetimes ranges from the picoseconds and up to almost the microseconds. Indeed, as shown in Table 1, only a four component decay time model originated a good fit (χ=1.20) with the following lifetimes: τ_1=657 ps; τ_2=10.0 ns; τ_3=59.42 ns; and τ_4=265 ns. The existence of relatively long lived components in dendrimer stabilized QDs (in the range of τ_3 and τ_4) has already been observed in studies using methanol as solvent [30, 32].

Figure 4 also shows the fluorescence time decay profiles in the presence of a quencher (nitromethane). The analysis of these decays shows that the longer lifetimes components are particular sensible to the presence of the quencher.

Table 1 Lifetime intensity decays of DAB-CdS nanoparticles in water without and in the presence of nitromethane

N	τ_i (ns)	B_i	P_i (%)	
Without nitromethane				
1	0.657(36)	0.726(7)	6.4	
2	10.0(4)	0.0845(7)	11.3	
3	59.42(8)	0.0430(2)	34.3	A=6.8(1)
4	265(2)	0.01350(4)	48.0	χ=1.20
[Nitromethane] = 0.00365 M				
1	0.514(33)	1.012(9)	8.3	
2	9.6(4)	0.0873(7)	13.4	
3	56.5(8)	0.04396(5)	39.6	A=6.2(1)
4	226(2)	0.011(9)	38.7	χ=1.17
[Nitromethane] = 0.0730 M				
1	0.77(4)	0.616(5)	11.7	
2	10.7(5)	0.0880(6)	23.2	
3	53.7(5)	0.0350(1)	46.1	A=8.82(8)
4	241(4)	0.00321(3)	19.0	χ=1.27
[Nitromethane] = 0.146 M				
1	0.58(3)	0.884(8)	15.2	
2	8.2(4)	0.0973(8)	23.9	
3	39.5(7)	0.0357(2)	42.1	A=3.24(8)
4	173(3)	0.00363(3)	18.7	χ=1.29
[Nitromethane] = 0.219 mol/L				
1	0.52(3)	0.987(9)	18.6	
2	7.2(4)	0.1086(9)	28.3	
3	32.2(7)	0.0345(2)	40.5	A=4.18(6)
4	130(3)	0.00264(4)	12.5	χ=1.27

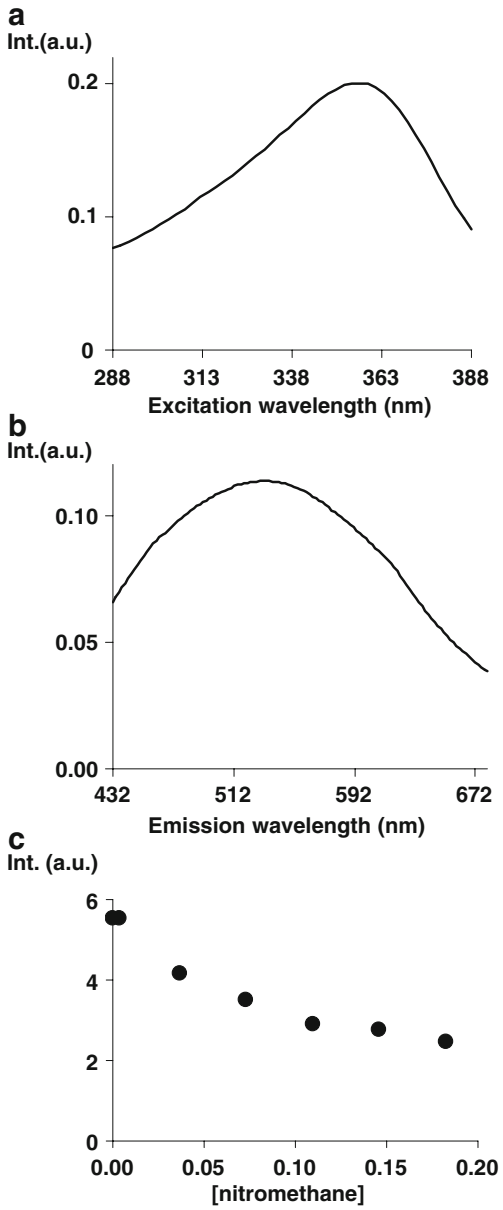

Fig. 5 PARAFAC estimation of the excitation (**a**) and emission spectra (**b**), and quenching profiles in the presence of nitromethane (**c**) of aqueous solutions of DAB-CdS

Table 1 shows the life times calculated with a four component decay time model when nitromethane is present. The analysis of Table 1 shows that when the concentration of nitromethane is increased the lifetimes of the longer lifetimes components as well as the correspondent fraction contribution decreases.

PARAFAC analysis of the quenching

As shown in Fig. 3, the presence of nitromethane provokes an overall decrease of the fluorescence of DAB-CdS. In order to analyze the structure of the EEM acquired as function of the nitromethane concentration, *i.e.* if besides quenching a shift of the emission or excitation wavelength is observed, PARAFAC analysis was done using different component models (from one and up to three components) [15, 16]. Typical values for the corcondia test (explained variance) for these three models were: one component, 100% (99.58%); two components, −11.78% (99.84%); and, three components, −0.24% (99.96%). These error parameters show that the intrinsic EEM model is constituted by one component [43], showing that only spectral variations due to quenching are observed.

Figure 5 shows typical results of the trilinear decomposition of sets of EEM collected in the presence of increasing amounts of nitromethane. Figure 5a shows the excitation and Fig. 5b shows the emission spectra. Figure 5c shows typical quenching profiles that are going to be analysed in the following section.

Quenching of the fluorescence of DAB-CdS by nitromethane

In order to analyze the quenching mechanism provoked by nitromethane, Stern-Volmer plots were done which shows a linear trend (Fig. 6a and Table 2). From these plots a Stern-Volmer constant of 9.0(4) M^{-1} can be estimated. This order of magnitude is compatible with a dynamic quenching (collisional) between the DAB-CdS and nitromethane.

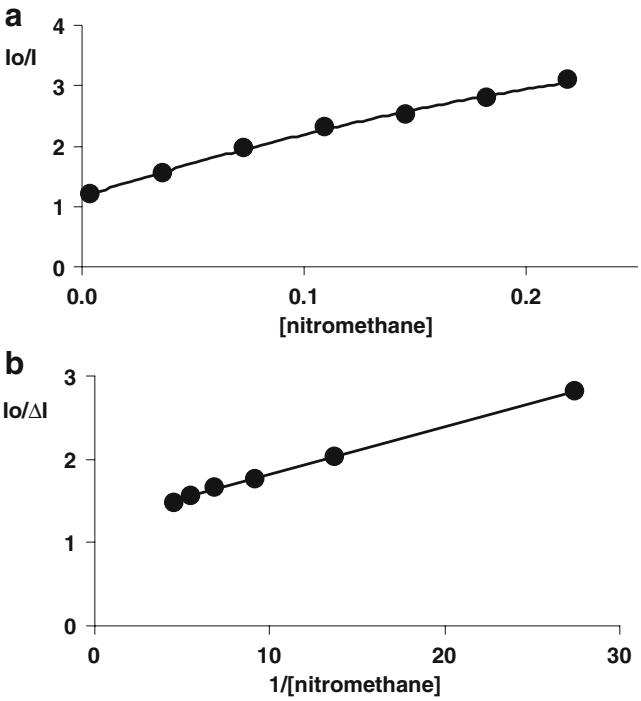

Fig. 6 Stern-Volmer plots of the quenching of the fluorescence of aqueous solutions of DAB-CdS by nitromethane

Table 2 Linear fitting parameters of the quenching profiles using Stern-Volmer models[a]

Model	K_D (M^{-1})	Intercept	f_a	R	Points	Concentration range (M)
Stern-Volmer	9.0(4)	1.32(5)		0.984	7	0.004–0.2
Modified Stern-Volmer	25(6)		0.81(4)	0.999	6	0.04–0.2

[a] Average and standard deviation of three independent experiments. f_a fraction of initial fluorescence that is accessible to nitromethane, *R* correlation coefficient, *Points* number of points used in the model linear fit

However, a detailed analysis of the Stern-Volmer plots shows the existence of a slightly downward curvature. This observation is supported by the calculated intercept, 1.32 (5), which is significantly higher than the expected unity, and suggests that the fluorophores dispersed on the dendrimer structure are not all accessible to the quencher (nitromethane) [45]. To assess this hypotheses a modified Stern-Volmer plot was done (Fig. 6b and Table 2) and, with this model, a better linear fitting of the quenching profiles as function of nitromethane concentration is achieved.

From the modified Stern-Volmer plots a Stern-Volmer constant of 25(6) M^{-1} is calculated and the percentage of fluorophores accessible to the quencher is about 81%. This result shows that about 19% of the CdS QDs (fluorophores) are located in the inner layers of the dendrimer while about 81% are located in the external layer of the dendrimer. As discussed above, the components with longer lifetimes are particularly sensible to the presence of nitromethane. As hypotheses one can associate these longer lifetimes components to those fluorophores that are located in the external lay of the dendrimer.

Conclusions

A fluorescent hybrid CdS QDs dendrimer nanocomposite synthesised in water and stable in aqueous solution is described. It is excited in the near UV and emits blue radiation. The fluorescence decay time profiles are complex and can be described using a four component model. It was observed that nitromethane is a collisional quencher of the fluorescence of the nanomaterial and it allow the estimation of the percentage of fluorophores accessible to the external chemical environment.

This nanomaterial is characterized by a relatively high Stokes' shift and has a high percentage of the fluorophores accessible to the external chemical environment characterized with a lifetime in the micromolar range. These set of favourable properties show that this nanomaterial has great potential as sensor.

Acknowledgments The authors would like to thanks the Fundação para a Ciência e Tecnologia (Lisboa, Portugal) under the frame of the Ciência 2007 program. Financial support from Fundação para a Ciência e Tecnologia (Lisboa, Portugal) (FSE-FEDER) (Project PTDC/QUI/71001/2006) and (Project PTDC/QUI/71336/2006) is acknowledged. C.M. Casado and B. Alonso (Departamento de Química Inorgánica, Facultad de Ciencias, Universidad Autónoma de Madrid, Spain) are acknowledged for providing samples of DAB dendrimers.

References

1. Alivisatos AP (1996) Semiconductor clusters, nanocrystals, and quantum dots. Science 271:933–937
2. Niemeyer CM (2001) Nanoparticles, proteins, and nucleic acids: biotechnology meets materials science. Angew Chem Int Ed Engl 40:4128–4158
3. Wu XY, Liu HJ, Liu JQ, Haley KN, Treadway JA, Larson JP, Ge NF, Peale F, Bruchez MP (2003) Immunofluorescent labeling of cancer markers Her2 and other cellular targets with semiconductor quantum dots. Nat Biotechnol 21:41–46
4. Jaiswal JK, Simon SM (2004) Potentials and pitfalls of fluorescent quantum dots for biological imaging. Tr Cell Biol 14:497–504
5. Gao X, Yang L, Petros JA, Marshall FF, Simons JW, Nie S (2005) In vivo molecular and cellular imaging with quantum dots. Curr Opin Biotechnol 16:63–72
6. Gerion G, Pinaud F, Williams SC, Parak WJ, Zanchet D, Weiss S, Alivisatos AP (2001) Synthesis and properties of biocompatible water-soluble silica-coated CdSe/ZnS semiconductor quantum dots. J Phys Chem B 105:8861–8871
7. Murphy CJ (2002) Optical sensing with quantum dots. Anal Chem 74:520A–526A
8. Costa-Fernández JM, Pereiro R, Sanz-Medel A (2006) The use of luminescent quantum dots for optical sensing. Tr Anal Chem 25:207–218
9. Chen Y, Rosenzweig Z (2002) Luminescent CdS quantum dots as selective ion probes. Anal Chem 74:5132–5138
10. Liang JG, Ai XP, He ZK, Pang DW (2004) Functionalized CdSe quantum dots asselective silver ion chemodosimeter. Analyst 129:619–622
11. Chen JL, Zhu CQ (2005) Functionalized cadmium sulfide quantum dots as fluorescence probe for silver ion determination. Anal Chim Acta 546:147–153
12. Chen J, Gao Y, Xu Z, Wu G, Chen Y, Zhu C (2006) A novel fluorescence array for mercury(II) ion in aqueous solution with functionalized dadmium selenide nanoclusters. Anal Chim Acta 577:77–84
13. Ali EM, Zheng Y, Yu H, Ying JY (2007) Ultrasensitive Pb^{2+} detection by glutathione-capped quantum dots. Anal Chem 79:9452–9458
14. Wang YQ, Ye C, Zhu ZH, Hu YZ (2008) Cadmium tellurium quantum dots as pH-sensitive probes for tiopronin determination. Anal Chim Acta 610:50–56

15. Leitão JMM, Gonçalves HMR, Mendonça C, Esteves da Silva JCG (2008) Multiway chemometric decomposition of EEM of fluorescence of CdTe quantum dots obtained as function of pH. Anal Chim Acta 628:143–154
16. Gonçalves HMR, Mendonça C, Esteves da Silva JCG (2009) PARAFAC analysisof the quenching of EEM of fluorescence of glutathione capped CdTe quantum dots by Pb(II). J Fluoresc 19:141–149
17. Wang C, Zhao J, Wang Y, Lou N, Ma Q, Su X (2009) Sensitive Hg (II) ion detection by fluorescent multilayer films fabricated with quantum dots. Sensor Actuator B Chem 139:476–482
18. Chang SQ, Dai YD, Kang B, Han W, Mao L, Chen D (2009) UV-enhanced cytotoxicity of thiol-capped CdTe quantum dots in human pancreatic carcinoma cells. Toxicol Lett 188:104–111
19. Kuo YC, Wang Q, Ruengruglikit C, Yu H, Huang Q (2008) Antibody-conjugated CdTe quantum dots for Escherichia coli detection. J Phy Chem C 112:4818–4824
20. Ballou B, Lagerholm C, Ernst LA, Bruchez MP, Waggoner AS (2004) Noninvasive imaging of quantum dots in mice. Bioconjug Chem 15:79–86
21. Toprak E, Balci H, Blehm BH, Selvin PR (2007) Three-dimensional particle tracking via bifocal imaging. Nano Lett 7:2043–2045
22. Tomalia DA, Baker H, Dewald JR, Hall M, Kallos G, Martin S, Roeck J, Ryder J, Smith P (1985) A new class of polymers: starburst-dendritic macromolecules. Polym J 17:117–132
23. Roovers J (2000) Advances in polymer science branched polymers II, vol. 143. Springer-Verlag, Berlin
24. Vogtle F, Richardt G, Werner N (2009) Dendrimer chemistry. Concepts, synthesis, properties, applications. Wiley-VCH, Weinheim
25. Gattas-Asfura KM, Leblanc RM (2003) Peptide coated CdS quantum dots as nanosensors for Cu^{2+} and Ag^{+} detection. Chem Commun 21:2684–2685
26. Pileni MP, Motte L, Petit C (1992) Synthesis of cadmium sulfide in situ in revers emicelles: influence of preparation modes on size; polydispersity, and photochemical reactions. Chem Mater 4:338–345
27. Gao Y, Reischmann S, Huber J, Hanke T, Bratschitsch R, Leitenstorfer A, Mecking S (2008) Encapsulating of single quantum dots into polymer particles. Colloid Polym Sci 286:1329–1334
28. Bawarski WE, Chidlowsky E, Bharali DJ, Mousa SH (2008) Emerging nanopharmaceuticals. Nanomedicine: Nanotech Biol Med 4:273–282
29. Sooklal K, Hanus LH, Ploehn HJ, Murphy CJ (1998) A blue-emitting CdS/Dendrimer nanocomposite. Adv Mater 10:1083–1087
30. Lakowicz JR, Gryczynski I, Gryczynski Z, Murphy CJ (1999) Luminescence spectral properties of CdS naoparticles. J Phys Chem 103:7613–7620
31. Lemon BI, Crooks RM (2000) Preparation and characterization of dendrimer-encapsulated CdS semiconductor quantum dots. J Am Chem Soc 122:12886–12887
32. Gayen SK, Brito M, Das BB, Comanescu G, Liang XC, Alrubaiee M, Alfano RR, González C, Byro AH, Bauer DLV, Balogh-Nair V (2007) Synthesis and optical spectroscopy of a hybrid cadmium sulfide-dendrimer nanocomposite. J Opt Soc Am B 24:3064–3071
33. Juan JY, Jun LY, Ping LG, Jie L, Feng WY, Qin YR, Tinga LW (2008) Forensic science intern. Application of photoluminescent CdS/PAMAM nanocomposites in fingerprint detection. Forensic Sci Intern 179:34–38
34. Wisher AC, Bronstein I, Chechik V (2006) Thiolated PAMAM dendrimer-coated CdSe/ZnSe nanoparticles as protein transfection agents. Chem Commun 15:1637–1639
35. Svenson S, Tomalia DA (2005) Dendrimers in biomedical applications-reflections on the field. Adv Drug Deliv Rev 57:2106–2129
36. Sánchez-Sancho F, Pérez-Inestrosa E, Suau R, Mayorga C, Torres MJ, Blanca M (2002) Dendrimers as carrier protein mimetics for IgE antibody recognition. Synthesis and characterization of densely penicilloylated dendrimers. Bioconjugate Chem 13:647–653
37. Bouldin KK, Menzel ER, Takatsu M, Murdock RH (2000) Diimide-enhanced fingerprint detection with photoluminescent CdS/dendrimer nanocomposites. J Forensic Science 45:1239–1242
38. Booksh KS, Kowalski BR (1994) Theory of analytical chemistry. Anal Chem 66:782A–791A
39. Harshman RA (1970) Foundations of the PARAFAC procedure: models and conditions for an "explanatory" multi-mode factor analysis. UCLA Working Papers Phonetics 16:1–84
40. Esteves da Silva JCG, Novais SAG (1998) Trilinear PARAFAC decomposition of synchronous fluorescence spectra of mixtures of the major metabolites of acetylsalicylic acid. Analyst 123:2067–2070
41. Esteves da Silva JCG, Leitão JMM, Costa FS, Ribeiro JLA (2002) Detection of verapamil drug by fluorescence and trilinear decomposition techniques. Anal Chim Acta 453:105–115
42. Olivieri AC, Arancibia JA, Muñoz de la Peña A, Durán-Merás I, Mansilla AE (2004) Second-order advantage achieved with four-way fluorescence excitation-emission-kinetic data processed by parallel factor analysis and trilinear least-squares. Determination of methotrexate and leucovorin in human urine. Anal Chem 76:5657–5666
43. Bro R, Kiers HAL (2003) A new efficient method to determining the number of components in PARAFAC models. J Chemometr 17:274–286
44. Jie G, Liu B, Pan H, Zhu JJ, Chen HY (2007) Anal Chem 79:5574–5581
45. Lakowicz JR (2006) Principles of fluorescence spectroscopy, 3rd edn. Springer, New York